Molecular Therapy
Original Article

# N6-methyladenosine demethylase FTO enhances chemo-resistance in colorectal cancer through SIVA1-mediated apoptosis

Ziyou Lin,[1,2] Arabella H. Wan,[1,3] Lei Sun,[2] Heng Liang,[2] Yi Niu,[2] Yuan Deng,[2] Shijia Yan,[2] Qiao-Ping Wang,[4] Xianzhang Bu,[2] Xiaolei Zhang,[2] Kunhua Hu,[3] Guohui Wan,[2] and Weiling He[1,5]

[1]Department of Gastrointestinal Surgery, The First Affiliated Hospital, Sun Yat-sen University, Guangzhou 510080, China; [2]National-Local Joint Engineering Laboratory of Druggability and New Drug Evaluation, National Engineering Research Center for New Drug and Druggability (Cultivation), Guangdong Province Key Laboratory of New Drug Design and Evaluation, School of Pharmaceutical Sciences, Sun Yat-sen University, Guangzhou 510006, China; [3]Zhongshan School of Medicine, Sun Yat-sen University, Guangzhou 510080, China; [4]School of Pharmaceutical Sciences (Shenzhen), Sun Yat-sen University, Guangzhou 510080, China; [5]Center for Precision Medicine, Sun Yat-sen University, Guangzhou 510080, China

**N6-methyladenosine ($m^6A$) is the most pervasive RNA modification and is recognized as a novel epigenetic regulation in RNA metabolism. Although the $m^6A$ modification involves various physiological processes, its roles in drug resistance in colorectal cancer (CRC) still remain unknown. We analyzed the RNA expression profile of $m^6A$/A (%) with MRM mass spectrometry in human 5-fluorouracil (5-FU)-resistant CRC tissues, and used the $m^6A$ RNA immunoprecipitation assay to validate the $m^6A$-regulated target. Our results have shown that the $m^6A$ demethylase FTO was up-regulated in human primary and 5-FU-resistant CRC. Depletion of FTO decreased cell growth, colony formation and metastasis in 5-FU-resistant CRC cells *in vitro* and *in vivo*. Mechanistically, we identified SIVA1, a critical apoptotic gene, as a key downstream target of the FTO-mediated $m^6A$ demethylation. The $m^6A$ demethylation of SIVA1 at the CDS region induced its mRNA degradation via a YTHDF2-dependent mechanism. The SIVA1 levels were negatively correlated with the FTO levels in clinical CRC tissues. Notably, inhibition of FTO significantly reduced the tolerance of 5-FU in 5-FU-resistant CRC cells via the FTO-SIVA1 axis, whereas SIVA1-depletion could restore the $m^6A$-dependent 5-FU sensitivity in CRC cells. In summary, our findings demonstrate a critical role of FTO as an $m^6A$ demethylase enhancing chemo-resistance in CRC cells, and suggest that FTO inhibition may restore the sensitivity of chemo-resistant CRC cells to 5-FU.**

## INTRODUCTION

Colorectal cancer (CRC) is one of the most malignant diseases in the gastrointestinal tract, and causes over 600,000 deaths annually worldwide.[1] Over the past decade, the incidence and mortality rates of CRC have substantially declined owing to the improvement in curative treatments including polypectomy, chemotherapy, targeted molecular therapy, and immunotherapy. However, drug resistance and metastasis are the major challenges for CRC treatment and limit therapeutic efficacy.[2] 5-Fluorouracil (5-FU) is the main chemotherapeutic treatment alone or combination with other chemotherapeutic agents for CRC patients; however, the majority of advanced CRC patients treated with 5-FU eventually suffer a relapse and generate 5-FU resistance.[3] Tremendous progress has demonstrated that epigenetic events, together with genetic alterations contribute to initiation and progression of CRC, and are involved in development of acquired chemo-resistance.[4,5] Use of epigenetic drugs in CRC with focus on the advantages of combination therapy over single chemotherapy represents a promising field for CRC treatment.

N6-methyladenosine ($m^6A$) RNA methylation, the most pervasive RNA modification in humans, acts as an emerging regulatory mechanism at the post-transcriptional level.[6] This modification is reversible and its functional components are mostly defined as writer, eraser, and reader proteins. The writer complex includes METTL3, METTL14, and WTAP, defined as $m^6A$ methyltransferase.[7,8] The eraser enzymes FTO and ALKBH5 mediate the reversal of $m^6A$ methylation,[9,10] while $m^6A$ methylated transcripts are recognized by reader proteins such as YTH family member,[11] HNRNPA2B1,[12] and IGF2BP.[13,14] Currently the $m^6A$ modification is shown to affect RNA stability, translation, and degradation.[15,16] Dysregulation of

Received 9 January 2022; accepted 25 October 2022;
https://doi.org/10.1016/j.ymthe.2022.10.012.

**Correspondence:** Arabella H. Wan, Department of Gastrointestinal Surgery, The First Affiliated Hospital, Sun Yat-sen University, Guangzhou, 510080, China
**E-mail:** elliehwann@gmail.com
**Correspondence:** Kunhua Hu, Zhongshan School of Medicine, Sun Yat-sen University, Guangzhou 510080, China
**E-mail:** hukunh@mail.sysu.edu.cn
**Correspondence:** Guohui Wan, School of Pharmaceutical Sciences, Sun Yat-sen University, Guangzhou, 510006, China
**E-mail:** wanguoh@mail.sysu.edu.cn
**Correspondence:** Weiling He, Department of Gastrointestinal Surgery, The First Affiliated Hospital, Sun Yat-sen University, Guangzhou, 510080, China
**E-mail:** hewling@mail.sysu.edu.cn

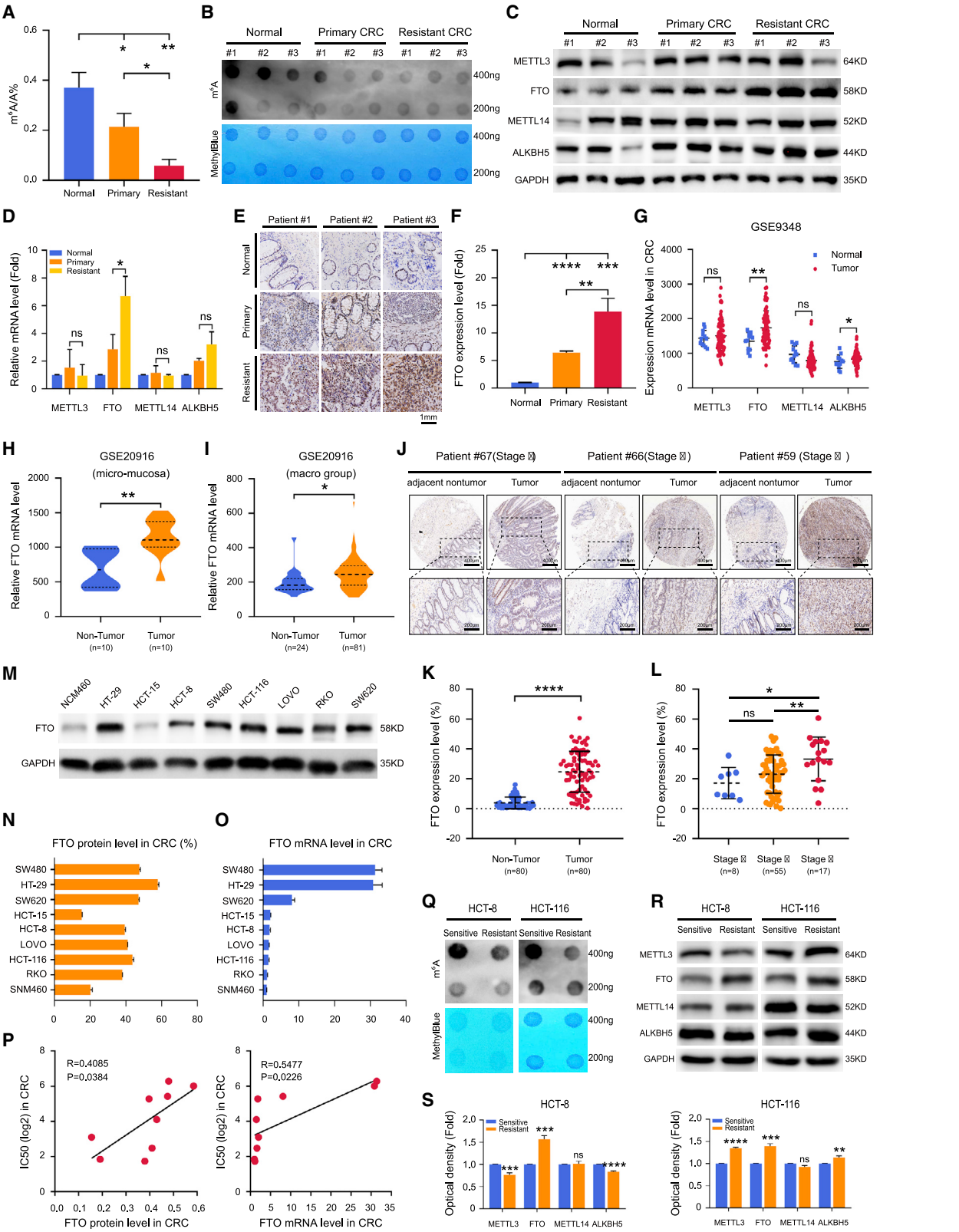


*(legend on next page)*

the m$^6$A levels is highly associated with tumor occurrence and progression.[17,18] Previous studies have reported that the m$^6$A modification is actively involved in chemo-resistance in various cancers, including head and neck squamous cell carcinoma, non-small-cell lung cancer, melanoma, and pancreatic cancer.[19-22] In a recent study, we reported that the m$^6$A writer methyltransferase-like 3 (METTL3) was down-regulated in sorafenib-resistant liver cancer via reducing the m$^6$A level of FOXO3 and enhancing FOXO3-mediated autophagy under hypoxia.[23] Emerging evidence has shown that the m$^6$A methylation plays an important role in mediating proliferation, migration, and metastasis in CRC[24-27]; however, whether m$^6$A modification is associated with drug resistance in CRC remains unclear.

Here, we aimed to investigate the role of m$^6$A modification in 5-FU-resistant CRC and explore the potential combination therapy with epigenetic drugs by targeting the m$^6$A methylation to improve CRC treatment. We found that FTO played an oncogenic role in CRC cell proliferation, colony formation, development, and progression *in vitro* and *in vivo*. Depletion of FTO enhanced the sensitivity of 5-FU-resistant CRC cells to 5-FU treatment via increasing the m$^6$A modification of SIVA1. Taken together, our findings provided novel insights into the significance of FTO status in predicting drug resistance in CRC patients, and the FTO-SIVA1 axis may be instrumental in CRC therapeutic treatment with 5-FU-based adjuvant chemotherapy.

## RESULTS

### Up-regulation of FTO in human primary and 5-FU-resistant CRC tissues

To explore the role of the m$^6$A modification in the acquired 5-FU resistance in CRC, we systematically analyzed the mRNA expression profile of m$^6$A/A (%) in normal, primary, and 5-FU-resistant tissues from CRC patients by multiple reaction monitoring (MRM) mass spectrometry. We found that the global m$^6$A levels were decreased in primary and 5-FU-resistant CRC tissues compared with normal tissues, with the lowest modification ratio of m$^6$A/A (%) in 5-FU-resistant CRC tissues (Figure 1A and Table S2). The reduced m$^6$A levels in primary and 5-FU-resistant CRC tissues were also confirmed by the dot-blotting assay (Figure 1B), suggesting a decreasing tendency of the m$^6$A levels during the progression of acquired 5-FU resistance in CRC. To examine the change of functional component in m$^6$A modification, we measured the key m$^6$A regulators in the tissues above and found that FTO was significantly up-regulated in 5-FU-resistant CRC tumors in both protein and mRNA levels (Figures 1C, 1D, and S1A), and up-regulation of FTO was also confirmed in the clinical CRC samples by immunohistochemistry assay (Figures 1E and 1F). In line with our results, up-regulation of FTO in CRC patients was validated by other independent clinical cohorts (Figures 1G and 1I). With analysis of the clinical outcome, we found that the up-regulated level of FTO showed poorer clinical prognosis in CRC patients (Figures S1B and S1C). The immunohistochemical (IHC) assay of clinical CRC patients demonstrated that FTO level was up-regulated in CRC tumor tissues compared with adjacent nontumor tissues (Figures 1J, 1K, and S1D). Moreover, the increased levels of FTO in CRC patients were significantly correlated with the higher pathological stages in our IHC assay and other database (Figures 1L and S1E).

To confirm the correlation between FTO and acquired 5-FU resistance, we first measured the expression of FTO at both protein and RNA levels in eight CRC cell lines and one normal colonic epithelial cell line (Figures 1M and 1O), and evaluated their sensitivity to 5-FU treatment (Figure S2A). Notably, the half maximal inhibitory concentration (IC50) of 5-FU was positively correlated with the expression levels of FTO in CRC cell lines (Figure 1P). To examine the direct role of FTO in the acquired 5-FU resistance, we overexpressed FTO in two CRC cells with lower level of FTO (RKO and HCT-15) and measured their response to 5-FU treatment. Overexpression of FTO triggered the increased tolerance toward 5-FU treatment in both RKO and HCT-15 cell lines (Figures S2B and S2C).

To mimic the acquirement of chemo-resistance in clinical, we generated the acquired 5-FU-resistant HCT-8 and HCT-116 cell lines by gradually increasing the concentration by 5% of IC50 until reaching to the IC50 (Figure S2D). Consistently, the global RNA m$^6$A levels were decreased in these 5-FU-resistant CRC cells, as indicated by both MRM mass spectrometry and the dot-blotting assay (Figure 1Q and Table S2). We found that the induction of FTO led to the change of the m$^6$A levels during the acquired resistance (Figures 1R, 1S, S2E, and S2F). Meanwhile, we further analyzed the variation of FTO

**Figure 1. Up-regulation of FTO in human 5-FU-resistant CRC**

(A) The m$^6$A/A ratio of the purified mRNA in normal, primary, and resistant tissues from CRC patients determined by MRM mass spectrometry assay, n = 3. (B) The m$^6$A level of global RNAs in normal, primary, and resistant tissues from CRC patients determined by dot-blotting assay. (C) The protein expression level of the m$^6$A regulator genes in normal, primary, and resistant tissues from CRC patients determined by western blotting assay. (D) The mRNA expression level of the m$^6$A regulator genes in normal, primary, and resistant tissues from CRC patients determined by RT-PCR assay. (E and F) Relative expression level of FTO in normal, primary, and resistant tissues from CRC patients determined by immunohistochemistry assay. Quantification was measured by Image Pro Plus (IPP) in (F). (G) The mRNA expression level of the m$^6$A regulator genes expression in human normal tissues (n = 12) and CRC tissues (n = 70) in GSE9348. (H and I) FTO expression level in human CRC tumors and nontumor tissues in GSE20916 with different groups: micro group derived from mucosa (H) and macro group (I). (J–L) FTO expression level of representative tumor and adjacent normal tissues in 80 pairs clinical CRC patients (J). Quantification of FTO expression level was measured by IPP in K (Tumor versus Nontumor) and L (different pathological Stage I-III). (M–O) The protein expression (M) and mRNA expression (O) of FTO in human CRC cell lines. NCM460 was human normal colon epithelial cell line as a control. Quantification of FTO protein level was measured by ImageJ in (N). (P) Pearson correlation analysis between FTO protein or mRNA level and the IC50 values of 5-FU in CRC cell lines. (Q) The m$^6$A level of global RNAs in HCT-8, HCT-8/5-FU, HCT-116, and HCT-116/5-FU cells by dot-blotting assay. (R and S) The protein expression level of the m$^6$A regulator genes in HCT-8, HCT-8/5-FU, HCT-116, and HCT-116/5-FU cells. Quantification was measured by ImageJ in (S). Data information: In all relevant panels, ns, no significant, *p < 0.05; **p < 0.01; ***p < 0.001; ****p < 0.0001; two-tailed t test. Data are presented as means ± SD and are representative of three independent experiments.

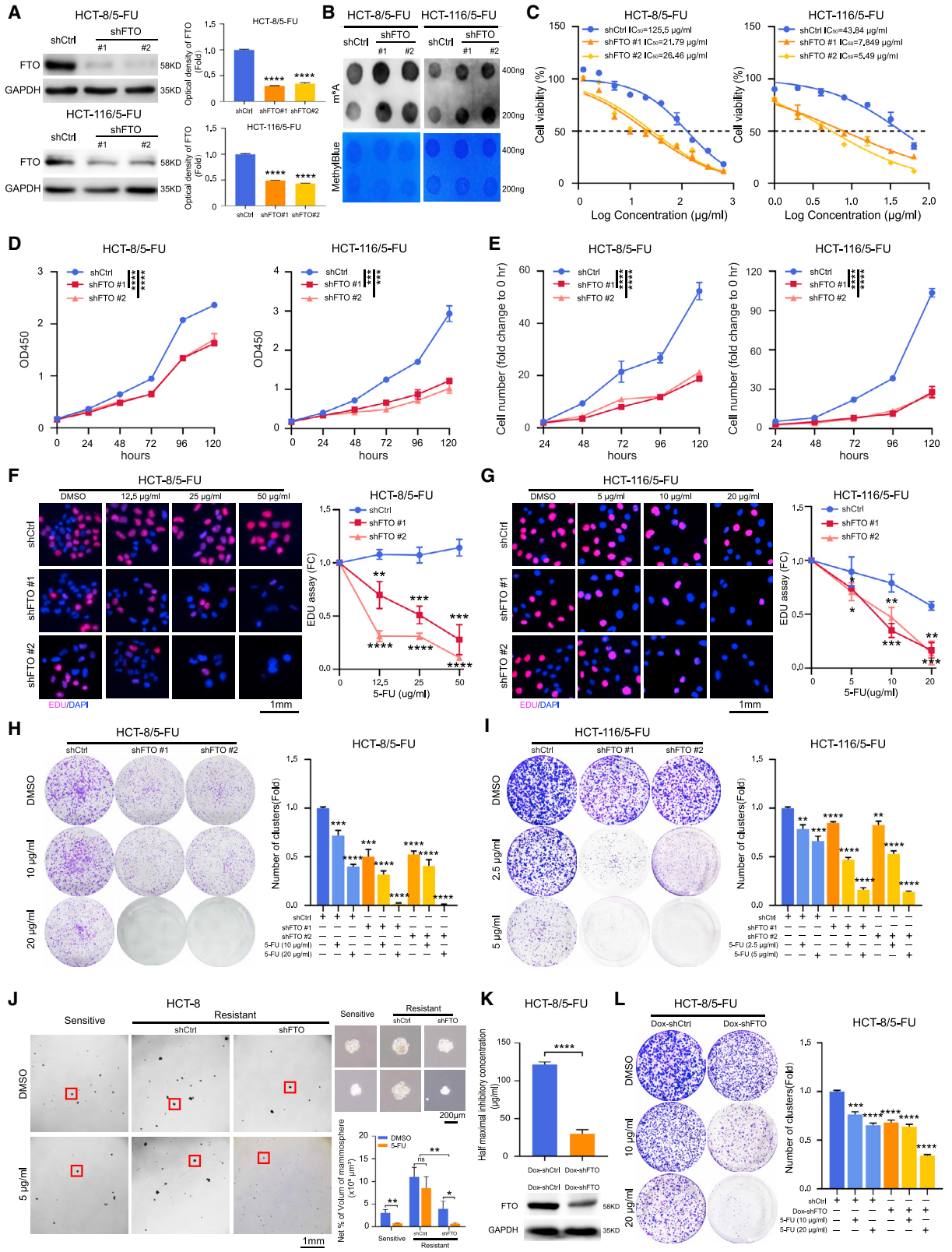


*(legend on next page)*

expression in HCT-8 naive and resistant cells treated with 5-FU for 24 h or 48 h from the GSE81005 database, and found that FTO was significantly up-regulated in resistant cells in 48 h treated with 5-FU (Figure S2G). However, the mRNA and protein expression levels of FTO had no change upon various doses of 5-FU treatment for 48 h from our cell model (Figures S2H–S2J). Overall, these data suggested the potential role of FTO-mediated $m^6A$ modification in 5-FU resistance in CRC.

### FTO promoted 5-FU resistance and cell growth in CRC cells

To validate the role of FTO in acquired 5-FU resistance, we constructed stable FTO-depleted CRC cell lines and verified by protein and mRNA expression levels (Figures 2A and S3A–S3C). We showed the decrease of global RNA $m^6A$ level in these stable FTO-depleted cell lines by dot-blotting assay (Figures 2B and S3D). Knockdown of FTO slightly up-regulated the level of ALKBH5, while the levels of METTL3 and METTL14 remained unchanged (Figures S3E and S3F). Notably, knockdown of FTO significantly increased the sensitivity of 5-FU (Figures 2C and S3G) and inhibited cell growth (Figures 2D, 2E, S3H, and S3I) in both naive and resistant HCT-8 and HCT-116 cell lines. Next, we confirmed the suppressed effect of FTO depletion in cell proliferation in a 5-FU dose-dependent manner by the EdU staining assay and the clonogenic survival assay (Figures 2F–2I and S3J–S3M). Furthermore, we performed the colonosphere formation assay by seeding control and FTO-depleted CRC cells in colonosphere culture medium with or without 5-FU treatment after 2 weeks of cultivation in non-adherent dishes. Knockdown of FTO in CRC cells dramatically impaired colonosphere formation and enhanced sensitivity to 5-FU treatment (Figures 2J and S4A). We also generated a doxycycline-inducible short hairpin RNA (shRNA) based-knockdown system for FTO in HCT8/5-FU cells to determine whether FTO affected CRC tumorigenesis (Figure 2K). Similarly, inducible-depletion of FTO by doxycycline suppressed cell proliferation in a 5-FU dose-dependent manner by the clonogenic survival assay (Figure 2L).

To verify the therapeutic potential of targeting FTO in 5-FU-resistant CRC, we used Rhein, a general FTO inhibitor to measure the suppressed effect of FTO (Figure S4B). Treatment with Rhein for 48 h caused down-regulation of FTO in a dose-dependent manner (Figure S4C), and induced the global RNA $m^6A$ levels in CRC cell lines accordingly (Figure S4D). Importantly, inhibition of FTO by Rhein restored the sensitivity of CRC cell lines toward 5-FU treatment (Figures S4E and S4F), as indicated with the suppression of cell colony formation (Figures S4G–S4J) and cell proliferation (Figures S4K–S4L). Since Rhein showed little selectivity for the ALKB subfamily, which may eclipse its utility for targeting FTO, we further used two more specific and selective FTO inhibitors, FB23 and FB23-2, to examine the therapeutic effects by inhibiting the activity of FTO (Figures S4M–S4P). Treatment with FB23-2 for 48 h caused the induction of global RNA $m^6A$ levels in 5-FU-resistant HCT-8 cells (Figure S4Q), and as expected, inhibition of FTO by FB23-2 could restore the sensitivity toward 5-FU treatment in HCT-8/5-FU cells (Figure S4R). Taken together, our results showed that FTO depletion enhanced the sensitivity to 5-FU and suppressed cell growth in CRC.

### Inhibition of FTO suppressed tumor growth and decreased 5-FU tolerance *in vivo*

To further confirm the role of FTO in inducing sensitivity of chemotherapy in colorectal cancer *in vivo*, we conducted two subcutaneous tumor xenograft models in BALB/C nude mice with inducible FTO-knockdown in HCT-8/5-FU and HCT-116/5-FU cell lines (Figures 3A and 3E). The Dox-shFTO CRC tumors showed increased sensitivity to 5-FU treatment compared with the Dox-Ctrl CRC tumors (Figures 3B, 3C, 3F, and 3G) and the knockdown effects by doxycycline were verified in tumors (Figures 3D, 3H, and 3I). Moreover, we used MC38, a mouse-derived CRC cell line, to generate the syngeneic mouse model. Knockdown of FTO in MC38 led to suppression on cell growth cell viability and colony formation *in vitro* (Figures S5A–S5F). Similarly, knockdown of FTO by shRNAs or inhibition of FTO by Rhein significantly enhanced the inhibitory effects of 5-FU treatment *in vivo*, as indicated by the reduced tumor size and tumor weight, while single treatment (Rhein or 5-FU) showed only slight suppression of tumor growth *in vivo* (Figures S5G–S5P).

In addition, we performed an intraperitoneal mouse model to mimic the microenvironment for colorectal tumors with inducible FTO-knockdown HCT8/5-FU cells or MC38 cells. As expected, the group treated with Dox-shFTO or FB23-2 in the Dox-system (Figures 3J–3M) and shFTO or Rhein in the shRNA-system (Figures S5Q and S5R) consistently showed increased sensitivity to 5-FU treatment compared with the control group. Analysis of tumor tissues by IHC verified that FTO depletion or FTO inhibition reduced the expression of Ki67, a marker of cell proliferation, and the reduction of Ki67 was more pronounced in the FTO-depletion group treated with 5-FU (Figures 3N and S5S).

**Figure 2. FTO enhanced 5-FU resistance, proliferation, colony formation in CRC cells**

(A) Stable FTO-knockdown in HCT-8/5-FU and HCT-116/5-FU cells by lentiviral shRNA sequences (shFTO#1 and #2). The knockdown effect was verified at protein level and quantification was measured by ImageJ on the right. (B) The $m^6A$ level of global RNAs in HCT-8/5-FU and HCT-116/5-FU cells with FTO-depletion. (C) Cell survival curves for FTO-knockdown in HCT-8/5-FU and HCT-116/5-FU cells treated with 5-FU for 48 h. (D) FTO-knockdown reduced cell growth determined by CCK8 assay in HCT-8/5-FU and HCT-116/5-FU cells. (E) FTO-knockdown reduced cell growth determined by cell numbers in HCT-8/5-FU and HCT-116/5-FU cells. (F–I) Knockdown of FTO increased the sensitivity of HCT-8/5-FU (F) and HCT-116/5-FU cells (G) to 5-FU after 48-h treatment by the EdU assay. Scale bar, 1 mm. (H and I) Knockdown of FTO decreased clonogenic survival of HCT-8/5-FU (H) and HCT-116/5-FU cells (I) treated with 5-FU for 10 days. (J) Knockdown of FTO impaired colonosphere formation in HCT-8 and HCT-8/5-FU cells. Scale bar, 1 mm. (K) Half maximal inhibitory concentration of FTO inducible-depletion in HCT-8/5-FU cells treated with 5-FU for 48 h. (L) Inducible-depletion of FTO decreased clonogenic survival of HCT-8/5-FU cells treated with 5-FU for 14 days. Data information: In all relevant panels, ns, not significant, $^*p < 0.05$; $^{**}p < 0.01$; $^{***}p < 0.001$; $^{****}p < 0.0001$; two-tailed t test. Data are presented as means ± SD and are representative of three independent experiments.

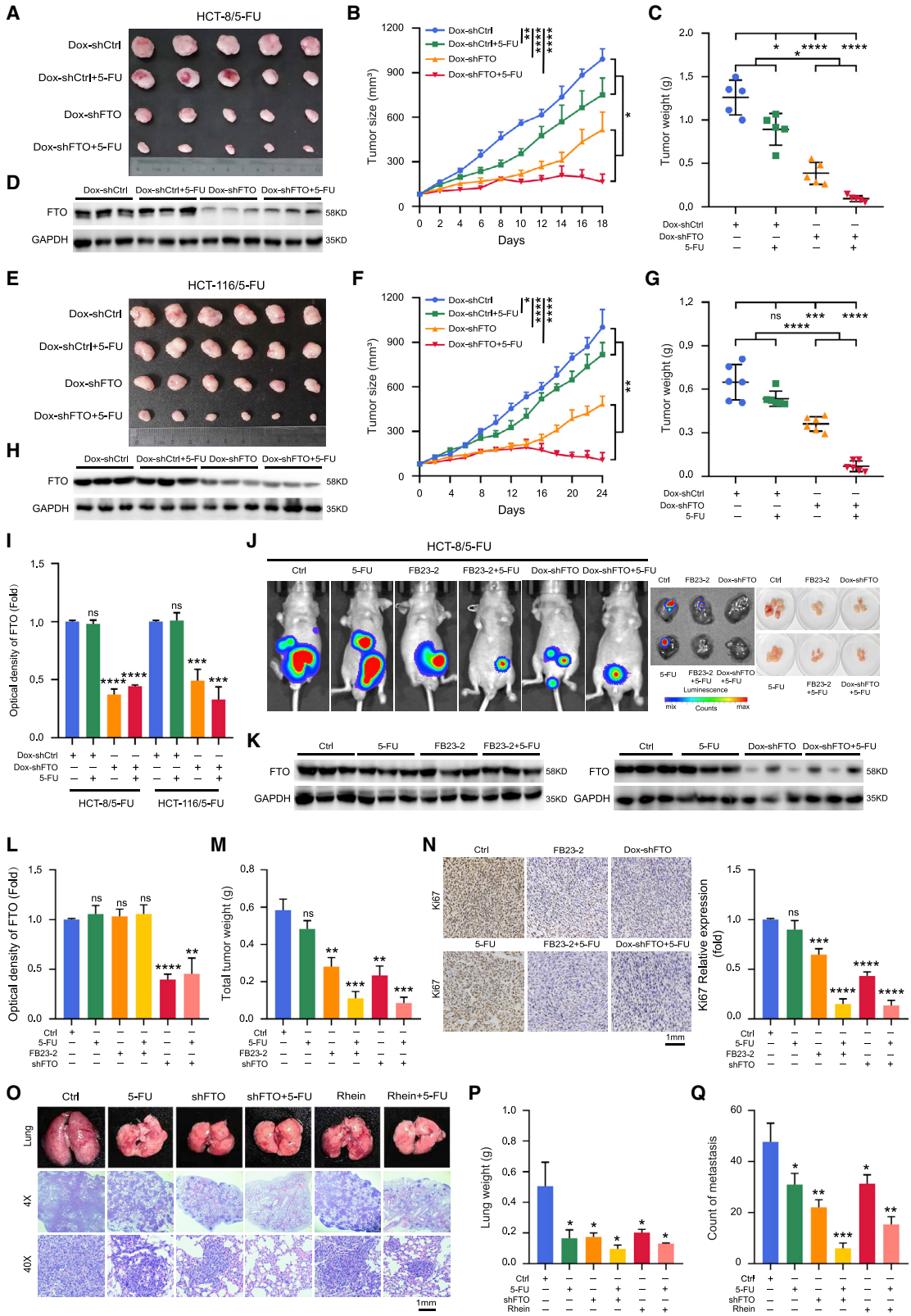


*(legend on next page)*

To investigate the effect on colorectal tumor metastasis, FTO-depleted MC38 cells and control cells were intravenously injected into C57BL/6 mice. As expected, silencing FTO attenuated lung metastasis and enhanced sensitivity to 5-FU in mice with the reduction of lung metastases and weight (Figures 3O–3Q). Collectively, these animal results suggested that FTO plays a critical role in promoting colorectal tumor growth and resistance to 5-FU *in vivo*.

### FTO regulated 5-FU resistance in CRC by mediating autophagic or apoptotic aberration

To explore how FTO mediated acquired 5-FU resistance in CRC, we examined the microenvironment with transmission electron microscopy in HCT-8/5-FU cells (Figure 4A). The number of autophagosomes in HCT-8/5-FU cells treated with 5-FU alone was increased compared with control, while the number of apoptosis bodies in HCT-8/5-FU cells with FTO depletion was increased regardless of 5-FU treatment. The positive correlation was found between the expression of LC3B, a marker of autophagy activation, and the expression of FTO in normal and 5-FU-resistant CRC tissues (Figures 4B–4D). Next, we examined autophagic activity by measuring the level of LC3 lipidation in FTO-knockdown CRC cell lines treated with various concentrations of 5-FU, and found that FTO depletion significantly reduced LC3-II accumulation (Figures 4E, 4F, 4H, and 4I). We used Chloroquine (CQ) to inhibit the late autophagy and measured the effects of FTO on the accumulation of LC3-II in CRC cells. FTO depletion caused inhibition of autophagy, as indicated by the weaker LC3 aggregation than the control (Figures 4G and 4J). In addition, we confirmed the reduction of autophagic signals with the subcellular redistribution of GFP-LC3 in CRC cell lines with FTO-knockdown or FTO inhibition by Rhein (Figures 4K–4N). Further, our results showed that knockdown of FTO resulted in significant increase of cell apoptosis and enhanced sensitivity to 5-FU treatment in CRC cell lines by flow cytometry (Figures 4O and 4P). The expression of Bcl-2, the biomarker of anti-apoptosis, was decreased under the treatment of 5-FU in FTO-knockdown cells compared with the control cells (Figures 4Q and 4R). It indicated that down-regulation of FTO may enhance apoptotic effect in CRC cells treated with 5-FU.

### FTO regulated apoptosis in CRC cells through mediating SIVA1 signaling

To explore the mechanism by which FTO regulates apoptosis, we performed qPCR array analysis in apoptotic signaling pathway and compared the apoptotic gene signatures in HCT-8 cells treated with or without FTO-knockdown (Figure 5A). Of note, the mRNA expression of SIVA1, an apoptotic inducing factor, was remarkably increased in FTO-knockdown cells. We confirmed the reduction of protein level of SIVA1 in both naive HCT-8 and HCT-8/5-FU cell lines with FTO depletion (Figures 5B and 5C). Knockdown of FTO increased the half-life of SIVA1 mRNA in HCT-8 cells (Figure 5D), indicating that the induction of SIVA1 may be caused by post-transcriptional regulation. To determine the potential $m^6A$ reader that regulated the expression of SIVA1, we first investigated the effect of knockdown of readers in the YTH family on SIVA1 mRNA expression in HCT8 cells by small interfering RNA (siRNA) and the results showed that the YTHDF1 or YTHDF2 may be the key binding protein affecting the mRNA stability of SIVA1 (Figures S6A and S6B). Next, we generated two stable cell lines with YTHDF1 knockdown and YTHDF2 knockdown (Figures S6C and S6D). Our results showed that knockdown of YTHDF2 increased both protein and mRNA levels of SIVA1 in FTO-knockdown cells, suggesting the role of FTO-mediated $m^6A$ modification in reducing SIVA1 expression in YTHDF2-dependent manner instead of YTHDF1 (Figures 5E–5G). Moreover, stable knockdown of YTHDF2 increased the half-life of SIVA1 mRNA in HCT-8 cells (S6E). In addition, knockdown of FTO significantly reduced the binding of YTHDF2 to SIVA1 mRNA analyzed by RNA immunoprecipitation (RIP)-qPCR (Figure 5H).

Since FTO is the core demethylase of RNA $m^6A$ modification, we analyzed the potential $m^6A$ sites in SIVA1 mRNA and identified two conserved motifs located in the coding sequence (CDS) from the metagene analysis in the GSE76414 database (Figures 5I and S6F). To explore the role of these two $m^6A$ sites in SIVA1, we generated two mutant forms of SIVA1 CDS by replacing A with T in the core motif (RRACH) of the potential $m^6A$ site (Figure 5J). The induction of SIVA1 protein level in FTO-knockdown cells was almost abolished in mutant #2 (Figure 5K), indicating the functional role of this $m^6A$ site mediated by FTO. To validate SIVA1 as a bona fide target of FTO for the $m^6A$ modification, we performed the $m^6A$-RIP assay (Me-RIP) and analyzed it with qRT-PCR. Knockdown of FTO significantly increased the $m^6A$ level of SIVA1 mRNA in mutant #2 site (Figure 5L). Moreover, we found the expression level of SIVA1 was negatively correlated with the expression level of FTO from the dataset of GSE30378 and TCGA (Figures 5M and 5N). We further validate their negative correlation in the MC38-hypodermic CRC models,

**Figure 3. Silencing FTO suppressed tumor growth and increased the sensitivity to 5-FU in CRC mouse models**

(A–D) Inducible-depletion of FTO effectively suppressed HCT-8/5-FU cell growth and increased the sensitivity to 5-FU *in vivo* (A). Tumor growth curve (B) and tumor weight (C) are shown. The effect of doxycycline-inducible FTO in tumors was determined by western blotting assay (D), n = 5. (E–H) Inducible-depletion of FTO effectively suppressed HCT-116/5-FU cell growth and increased the sensitivity to 5-FU *in vivo* (E). Tumor growth curve (F) and tumor weight (G) are shown. The effect of doxycycline-inducible FTO in tumors was determined by western blotting assay (H), n = 6. (I) Quantification of FTO expression in (D) and (H) by ImageJ. (J–N) Combination therapy with FTO inhibitor FB23-2 and 5-FU effectively suppressed HCT8/5-FU cell growth in intraperitoneal mice model (J). FTO expression in tumors was determined by western blotting assay (K and L). Tumor weight was quantified (M). Immunohistochemical images of Ki67 confirmed the tumor status in mice (N). (O–Q) Combination therapy with FTO inhibitor Rhein and 5-FU decreased lung metastases. Formation of CRC metastatic foci in the lung was confirmed by H&E staining (O). Lung weight was quantified after 2 weeks (P) and the count of metastases is shown in (Q). Data information: In all relevant panels, ns, not significant, *p < 0.05; **p < 0.01; ***p < 0.001; ****p < 0.0001; two-tailed t test. Data are presented as means ± SD.

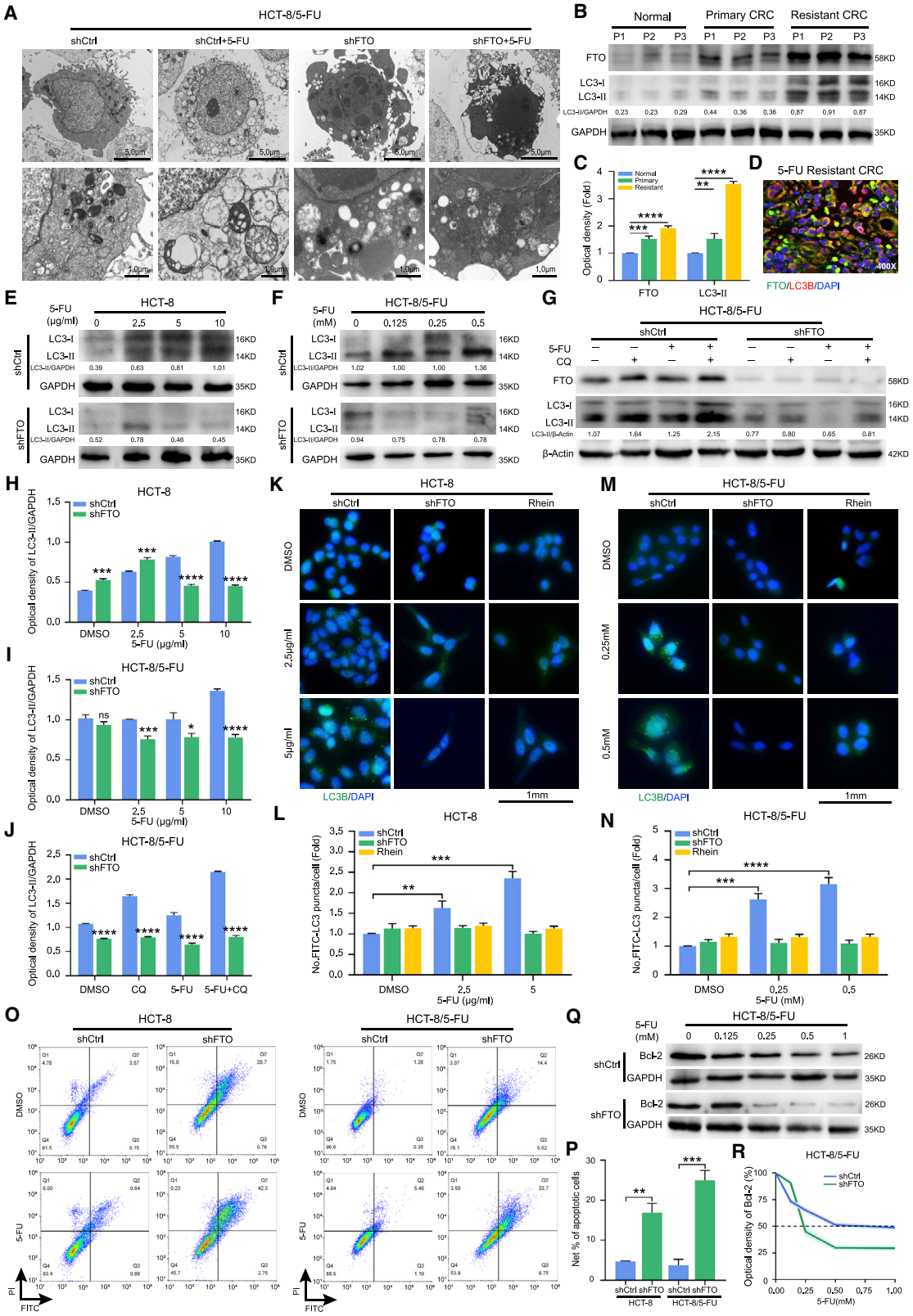


*(legend on next page)*

where knockdown of FTO or inhibition of FTO with Rhein resulted in decreased expression level of SIVA1 by IHC assay (Figure 5O). Collectively, we identified SIVA1 as a major downstream target of FTO in mediating apoptosis in CRC cells.

### Silencing SIVA1 significantly alleviated FTO-dependent tumor growth and tolerance *in vitro* and *in vivo*

To investigate whether SIVA1 played a crucial role in FTO-dependent tumor growth and progression, we first generated distinct shRNAs targeting SIVA1 and overexpression of SIVA1 in naive and HCT-8/5-FU cells, respectively (Figures S7A and S7B). SIVA1-depletion slightly increased cell proliferation while, conversely, overexpression of SIVA1 slightly inhibited cell proliferation (Figures S7C and S7D). Next, we generated distinct shRNAs targeting SIVA1 in FTO stable knockdown CRC cell lines (Figure 6A, S7E, and S7F). Knockdown of SIVA1 significantly desensitized the FTO-depletion-mediated susceptibility to 5-FU treatment and enhanced the IC50 values (Figure 6B). Silencing SIVA1 effectively rescued the growth of FTO-depletion in naive and HCT-8/5-FU cell lines (Figures 6C and 6D). In addition, we performed the clonogenic survival assay by seeding shCtrl, shFTO, and shFTO&shSIVA1 CRC cell lines treated with or without 5-FU and found that double knockdown shFTO&shSIVA1 CRC cell lines rescued colony formation compared with FTO-knockdown cells (Figures S7G and S7H). To define the direct role of the FTO-SIVA1 axis in the apoptosis pathway, the co-expression by the string analysis indicates that SIVA1 was highly related to the apoptotic biomarkers Bcl-2 and caspase-3 (Figure S7I). Knockdown of SIVA1 could rescue the FTO-deletion-mediated cell apoptosis by flow cytometry (Figures 6E and S7J). We also confirmed that knockdown of SIVA1 could rescue the expression of Bcl-2 in FTO-depleted CRC cell lines (Figures 6F, 6G, and S7K–S7L), as well as restore the inhibition of caspase-3 activity in FTO-depleted CRC cell lines under 5-FU treatment (Figures 6H–6J).

In addition, we performed subcutaneous implantation with stable shFTO and shFTO&shSIVA1 MC38 cells into the C57BL/6 mice (Figures 6K and S7M). Consistent with *in vitro* study, knockdown of SIVA1 and FTO promoted CRC tumor growth and significantly desensitized the FTO-depletion mediated susceptibility to 5-FU treatment in mice (Figures 6L and 6M). To explore whether the FTO-SIVA1 axis has therapeutic effects *in vivo*, we performed a CRC patient-derived xenograft (PDX) model in nude mice and administered with four regimens (Figure 7A). Notably, inhibition of FTO by Rhein significantly decreased PDX tumor growth and the tolerance to 5-FU (Figures 7B–7D), as indicated by the reduced tumor size and tumor weight. Inhibition of FTO increased the expression of SIVA1 in combination therapy with 5-FU treatment (Figure 7E), as shown as decreased cell proliferation (Ki67 expression) and increased apoptosis (Bcl-2 and caspase-3 expression) (Figures 7F–7I). Further, by analysis of R2 datasets, we revealed that SIVA1 levels are positively correlated with overall survival in CRC patients (Figures 7J and 7K). Taken together, these results demonstrated that silencing SIVA1 could significantly alleviate the inhibitory effects on tumor growth and tolerance of 5-FU mediated by FTO depletion *in vitro* and *in vivo*. Targeting the FTO-SIVA1 axis may have therapeutic potential to treat CRC patients with 5-FU resistance.

## DISCUSSION

N6-methyladenosine ($m^6A$) is a pervasive nucleotide modification in mRNA and was closely related with various human diseases including cancers.[17] FTO, the fat mass and obesity-associated protein,[28] is the first enzyme that identified as $m^6A$ demethylase,[9] and plays a critical role in mRNA stability[29] and various human diseases including cardiovascular diseases,[30] diabetes,[31] Alzheimer's disease,[32] and cancers.[33-36] Previously, Li et al. found the oncogenic role of FTO in regulating expression of ASB2 and RARA by reducing $m^6A$ levels in acute myeloid leukemia (AML).[37] Inhibition of FTO suppressed glioblastoma stem cell growth and self-renewal.[38] Targeting FTO emerges as a promising strategy for cancer treatment. Su et al. showed that R-2HG inhibited proliferation and survival of FTO-high AML cancer cells which in turn down-regulated the stability of MYC/CEBPA transcripts.[39] Recently, the dynamic $m^6A$ modification was reported as a critical epigenetic driver for TKI-tolerance in AML and sorafenib-tolerance in liver cancer.[23,40] However, the regulation of $m^6A$ modification in mediating acquired drug resistance in CRC remains unknown.

Recently, Ruan et al. demonstrated that FTO down-regulation mediated by hypoxia promoted CRC metastasis via inhibiting metastasis-associated protein 1 (MTA1) expression, suggesting a potential tumor suppressive role of FTO in CRC.[41] Another study conducted by Relier et al. also showed the beneficial role of low level of FTO in CRC in which FTO was shown to inhibit cancer stem cell abilities by an

**Figure 4. The switched role of FTO in mediating autophagy and apoptosis in CRC cells**

(A–C) Electron micrographs of 5-FU-resistant HCT-8 cells with FTO-knockdown. Scale bar, 5.0 μm and 1.0 μm. (B and C) Protein level of LC3 I/II and FTO in normal, primary, and resistant tissues from CRC patient (B). Quantification was measured by ImageJ in (C).

(D) The heterogeneity of 5-FU-resistant CRC tumors. FTO and LC3B protein expression was measured by immunofluorescent microscopy. Scale, 400X. (E and F) Knockdown of FTO reduced protein levels of LC3 I/II in HCT-8 (E) and HCT-8/5-FU cell lines (F) treated with 5-FU for 24 h. (G) Knockdown of FTO reduced accumulation of LC3-II in HCT-8/5-FU cell lines treated with 5-FU (0.25 mM) or Chloroquine (50 μM) for 24 h. (H–J) Quantification of LC3 II/GAPDH in (E), (F), and (G) was measured by ImageJ, respectively.

(K–N) Knockdown or inhibition of FTO decreased the LC3 levels in HCT-8 (K) and HCT-8/5-FU (M) cell lines treated with 5-FU for 24 h by immunostaining assay. Quantification was measured by Imaris in (L) and (N), respectively. (O and P) Knockdown of FTO increased cellular apoptosis in HCT-8 and HCT-8/5-FU cell lines treated with 5-FU for 24 h by fluorescence-activated cell sorting. Net percentage of apoptotic cells is shown in (P). (Q and R) Knockdown of FTO down-regulated Bcl-2 expression level in HCT-8/5-FU cells treated with 5-FU for 24 h. Optical density of Bcl-2 was quantified by ImageJ in (R). Data information: In all relevant panels, ns, not significant, *$p < 0.05$; **$p < 0.01$; ***$p < 0.001$; ****$p < 0.0001$; two-tailed t test. Data are presented as means ± SD and are representative of three independent experiments.

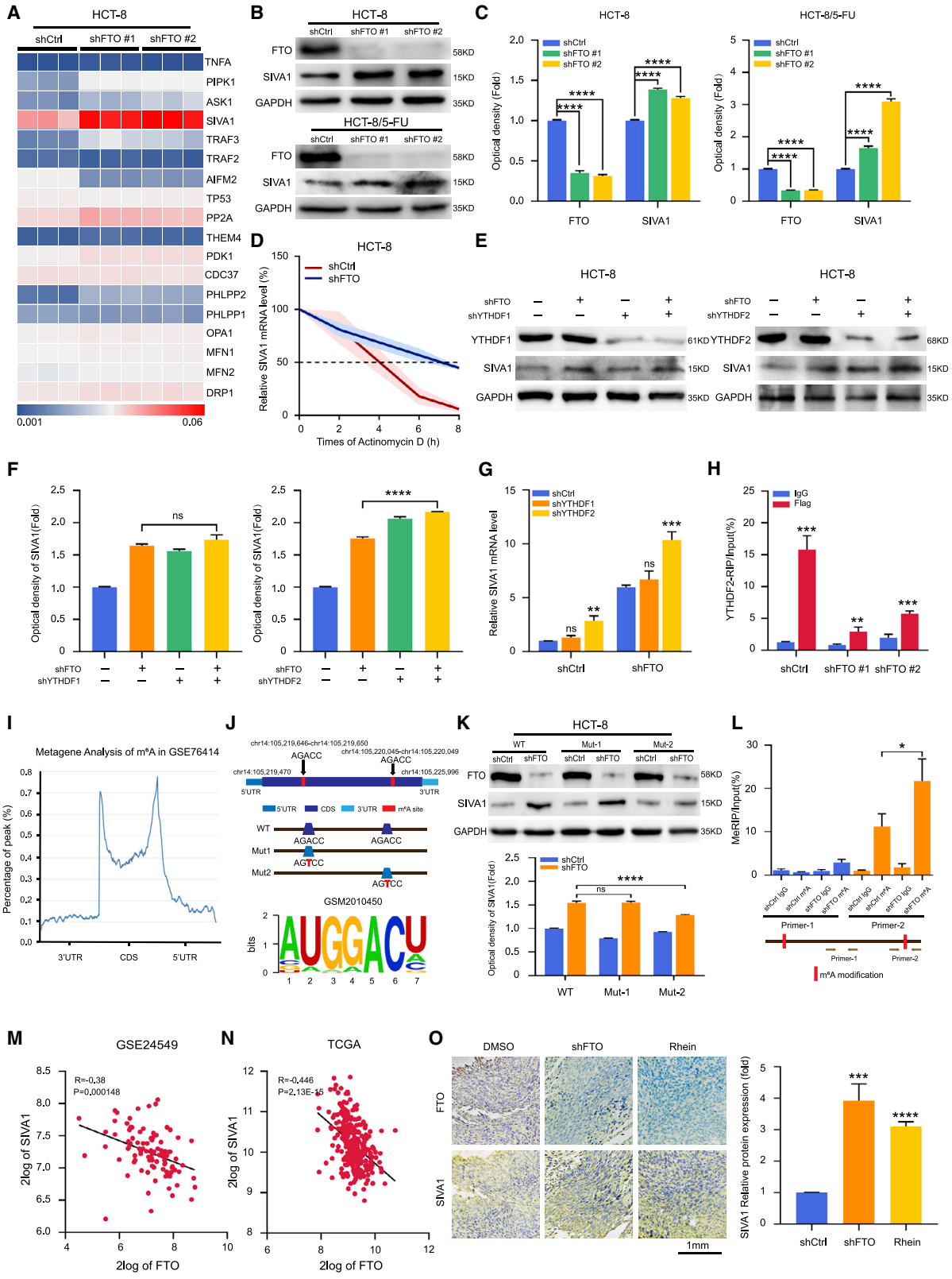


*(legend on next page)*

axis of FTO/PCIF1/CAPAM through $m^6A_m$ modification.[42] However, a recent study identified an oncogenic role of FTO in CRC by demethylating G6PD/PARP1 and suggested targeting FTO could block CRC tumor growth and reversed chemotherapy resistance.[43] These studies raised a controversial role of FTO in CRC and provided an open view on the regulatory role of $m^6A$ modification under various physiological conditions. In our study, we systematically analyzed the expression of FTO in several CRC databases, and found that FTO may play an oncogenic role in CRC chemo-resistance. The expression level of FTO could be reflected in the severity of the CRC patients and the higher expression level of FTO was significantly associated with poorer clinic prognosis in some public databases, indicating the oncogenic role of FTO in mediating chemo-resistance for CRC. We further confirmed that FTO was up-regulated in primary and 5-FU resistant CRC tumors compared with the adjacent nontumor tissues. Overexpression of FTO in CRC cells increased their tolerance toward 5-FU treatment. Depletion of FTO significantly decreased cell proliferation, metastasis, and tumorigenesis in CRC. More importantly, inhibition of FTO by Rhein could restore sensitivity of 5-FU-resistant CRC cells to 5-FU treatment. Rhein is the first potent compound extracted from Polygonaceae Rheum Officinale that competitively binds to the FTO active site to inhibit the activity of $m^6A$ demethylation.[44] Our results demonstrated that Rhein could decrease cell proliferation, colony formation, metastasis, and tumor growth even though the inhibitory effect was weaker than that of the treatment with shRNA. Since Rhein shows little selectivity for the ALKB subfamily, more potent and effective FTO inhibitors have been under development. Recently, Huang et al. reported two promising FTO inhibitors named as FB23 and FB23-2, which directly bind to FTO and selectively inhibit FTO-mediated $m^6A$ demethylase activity and showed good antitumor effects *in vivo*.[45] We also demonstrated that FB23-2 could increase the sensitivity of CRC cells to 5-FU both *in vitro* and *in vivo*. Subsequently, Peng et al. identified entacapone as a potential FTO inhibitor based on a structure virtual screening,[46] and Su et al. developed two more potent FTO inhibitors (CS1 and CS2) and proved that these inhibitors could suppress cancer stem cell maintenance and immune evasion.[47] Compared with FB23-2, the novel FTO inhibitors CS1 and CS2 showed lower IC50 value toward treatment of AML and other cancers, which may present a broad and effective treatment for chemo-resistant CRC.

Currently, tolerance to chemotherapy and targeted therapies is a major barrier in cancer treatment. Liu et al. identified that the $m^6A$ methylation played a crucial role in regulating cell fate decisions and demonstrated that dynamic $m^6A$ methylome was an additional epigenetic driver of reversible TKI-tolerance state.[48] Yang et al. found that FTO promoted melanoma tumorigenesis and mediated melanoma resistance to anti-PD-1 *in vitro* and *in vivo*. In their study, FTO level was increased in human melanoma induced by metabolic starvation stress and knockdown of FTO sensitized melanoma cells to interferon gamma (IFN-γ) and sensitized melanoma to anti-PD-1 treatment via adaptive immunity. Importantly, the combination of FTO inhibition with anti-PD-1 blockade can reduce the resistance to immunotherapy in melanoma.[21] Our recent study also found that reduced RNA $m^6A$ methylation promoted sorafenib resistance in hepatocellular carcinoma through FOXO3-mediated autophagy.[23] For CRC, few studies have focused on the role of $m^6A$ modification in regulating tolerance to chemotherapeutics. Here, we first demonstrated that FTO played a switch role in sensitivity to 5-FU treatment in CRC, which enhanced tolerance via activating the autophagy signaling pathway in 5-FU-resistant CRC and decreased tolerance via following apoptosis signaling pathway in primary CRC. Previous studies have shown that autophagy performed as a protective mechanism in development of tolerance of chemotherapeutics.[49-52] Consistently, we found up-regulation of FTO promoted LC3B accumulation in 5-FU-resistant CRC cells. Consequently, depletion of FTO accelerated the process of apoptosis and inhibited the tumor growth in both primary and 5-FU-resistant CRC cell lines.

To decipher the molecular mechanism by which FTO-mediated $m^6A$ modification regulated apoptosis, we performed analysis in the apoptotic signaling pathway and identified SIVA1 as the downstream of FTO-mediated apoptosis in CRC. SIVA1 was previously shown to bind to and inhibit Bcl-mediated protection against UV radiation-induced apoptosis.[53] As an apoptosis-inducing factor, SIVA1 was involved in CD27-mediated apoptosis[54] and p53-mediated apoptosis.[55] In this study, silencing FTO promoted SIVA1 expression in both mRNA and protein levels. We further identified two potential $m^6A$ sites in the CDS region of SIVA1 from Metagene analysis and verified that the site located at chr14:105,220,045-chr14:105,220,049 was the essential site to modulate the stability of SIVA1 mRNA by Me-RIP analysis. In addition, we investigated the role of potential $m^6A$ readers in mediating the SIVA1 mRNA expression.[12,16] Previous studies have shown that YTHDF2 can destabilize the target mRNA via promoting mRNA degradation.[56-58] Here, our results showed that FTO mediated-$m^6A$ modification decreased SIVA1 expression

**Figure 5. SIVA1 as a downstream target of FTO-mediated $m^6A$ modification in CRC**

(A) Heatmap of differentially expressed genes involved in apoptotic signaling pathway in FTO-knockdown HCT-8 cells. (B and C) Protein level of SIVA1 in FTO-knockdown HCT-8 and HCT-8/5-FU cell lines. Quantification was measured by ImageJ in (C). (D) Half-life of SIVA1 mRNA in FTO-knockdown HCT-8 cells treated with actinomycin D. (E and F) Protein level of SIVA1 in FTO-knockdown naive HCT-8 cells was affected by the $m^6A$ binding proteins YTHDF1 (E) and YTHDF2 (F). Quantification was measured by ImageJ in (F). (G) The mRNA level of SIVA1 in FTO-knockdown naive HCT-8 cells was affected by the $m^6A$ binding proteins.

(H) Knockdown of FTO reduced the $m^6A$ methylation in SIVA1 mRNA by the YTHDF2-RIP analysis. (I) Metagene analysis of $m^6A$ site in SIVA1 based on GSE76414 database. (J) Mutation of the $m^6A$ consensus sequence was generated by replacing adenosine with thymine. (K) Protein in the wild-type form and mutant form of SIVA1 in FTO-knockdown HCT-8 cells. (L) The $m^6A$ Me-RIP analysis of SIVA1 in FTO-knockdown HCT-8 cells. (M) Pearson correlation between FTO and SIVA1 mRNA expression in GSE30378. (N) Pearson correlation between FTO and SIVA1 mRNA expression in TCGA-COAD. (O) The correlation of SIVA1 expression and FTO expression level in MC38-hypodermic CRC tumor treated with Rhein or FTO shRNA. Data information: In all relevant panels, ns, not significant, $^*p < 0.05$; $^{**}p < 0.01$; $^{***}p < 0.001$; $^{****}p < 0.0001$; two-tailed t test. Data are presented as means ± SD and are representative of three independent experiments.

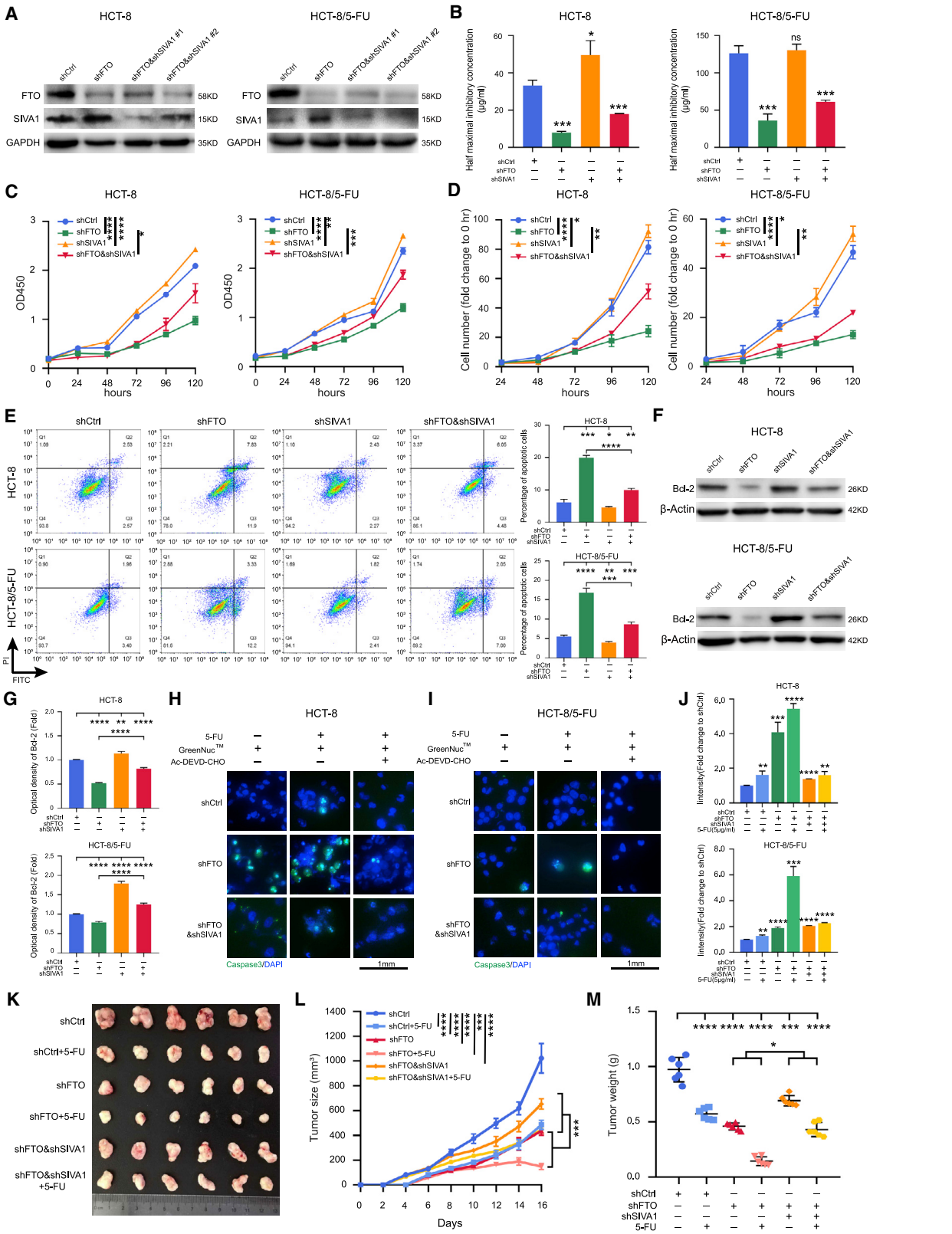


*(legend on next page)*

in the YTHDF2-dependent manner in CRC. Depletion of SIVA1 in FTO-knockdown CRC cells could effectively rescue the suppression of cell proliferation, colony formation, and susceptibility to 5-FU treatment in CRC. However, all the alleviations induced by SIVA1 were limited compared with the same treatment to the control CRC cells, which suggested that there may be other underlying mechanisms involved in FTO-mediated $m^6A$ modification.

In summary, we have demonstrated that FTO was up-regulated in development of 5-FU resistance in CRC cells. Inhibition of FTO suppressed CRC tumorigenicity through FTO-mediated $m^6A$ modification in SIVA1 mRNA decay in a YTHDF2-dependent manner (Figure 7L). Inhibition of FTO restored sensitivity of 5-FU treatment in 5-FU-resistant CRC cells. Our findings suggested that FTO may be a potential therapeutic target in CRC and combination therapy of FTO inhibitors and chemotherapy may be an effective strategy for resistant CRC treatment.

## MATERIALS AND METHODS

### Tissue and cell culture

The CRC patient samples were obtained at the First Affiliated Hospital of Sun Yat-sen University and were approved by the institutional review board of the hospital. The study was compliant with all relevant ethical regulations regarding research involving human participants. HCT-8, HCT-116, HEK-293T, and MC38 cells were obtained from the Procell. All cells were cultured in RPMI-1640 or DMEM (Corning, USA) with 10% fetal bovine serum at 37°C in 5% $CO_2$. All cell lines were stored in multiple back up upon receipt to reduce risk of phonotypic drift, and tested with mycoplasma free by Mycoplasma Stain Assay Kit (C0296, Beyotime, China). Cell line authentication was validated by the STR analysis using GenePrint 10 System according to the manufacturer's instruction (B9510, Promega, USA). 5-FU-resistant HCT-8 and HCT116 cell lines were generated by exposing the cells with 5-FU at 5% of IC concentration for 3 days and gradually increased the concentration by 5% of IC until reaching the IC50.

### Multiple reaction monitoring mass spectrometry

RNA sample (10 μg) was digested with nuclease P1 (Sigma, USA) enzyme at 37°C for 1 h, and subsequently incubated with alkaline phosphatase (Sigma, USA) at 37°C for 4 h. The digested products were diluted and analyzed directly with SCIEX Triple Quad 4500 liquid chromatography-tandem mass spectrometry system and SCIEX ExionLC AC UHPLC system. The control software was analyst 1.6.3 and all the data were quantified with Multiquant.

### Plasmid constructions, cell transfection, and virus infection

Stable knockdown of target genes was accomplished by lentiviral-based specific shRNA delivery. For inducible knockdown of FTO, the FTO shRNAs were cloned into the Tet-on pLKO.1 vector (21,915, Addgene). The vector pLKO.1-puromycin or pLKO.1-hygromycin was constructed by using primers listed in Table S1. The SIVA1 cDNA clone (NM_006427) was constructed into pcDNA3.1 vector, and two mutant forms SIVA1 were generated from A to T by QuikChange II Site-Directed Mutagenesis Kit (200,523, Agilent, USA) according to the instructions. For stable knockdown assay, pLKO.1 vector together with packing and helper plasmids PAX2 and MD2G were co-transfected into HEK-293T cells by Calcium Phosphate Transfection Kit (CAPHOS-1KT, Sigma). Viruses were produced, filtered, and titrated according to the instruction, and infected the desired cells with 8 μg/mL Polybrene (TR-1003, Sigma). After screening by puromycin (1–5 μg/mL) or hygromycin (100 μg/mL) in corresponding concentration for 3 to 5 days, the stable knockdown or overexpression cells were harvested and analyzed by immunoblot or qPCR assay.

### Antibodies

Anti-METTL3 (western blot [WB] 1:1,000; IHC 1:500; ab195352), anti-FTO (WB 1:1,000; IHC 1:500; ab124892), anti-METTL14 (WB 1:1,000; IHC 1:500; ab220030), anti-ALKBH5 (WB 1:1,000; IHC 1:500; ab174124), goat anti-rabbit immunoglobulin (Ig)G (WB 1:2000; ab6721) and goat anti-rabbit IgG-FITC (immunofluorescence [IF] 1:200, ab6717) antibodies were purchased from Abcam, USA. Anti-MAP1LC3-B (WB 1:1,000; IHC 1:100; IF 1:100; A7198), anti-MAP1LC3-B (WB 1:1,000; IHC 1:100; IF 1:100; A7198), anti-Bcl-2 (WB 1:1,000; IHC 1:100; A), anti-YTHDF1(WB 1:1,000; IHC 1:100; A18126), anti-YTHDF2 (WB 1:1,000; IHC 1:100; A15616), anti-Ki67 (IHC 1:100; A11390), anti-GAPDH (WB 1:1,000; AC027) and anti-β-actin (WB 1:50,000; AC026) antibodies were purchased from Abclonal, China. Anti-$m^6A$ (Me-RIP 1:1,000; ABE572) antibody was purchased from Merck Millipore (Massachusetts, USA). Western blot analyses were performed by standard methods described previously.[59]

### Quantitative RT-PCR

Total RNA was isolated using Trizol reagent according to the manufacturer's instruction (ThermoFisher, USA) and the cDNA was

**Figure 6. Silencing SIVA1 alleviated FTO-dependent tumor growth *in vitro* and *in vivo***

(A) Protein level of SIVA1 in FTO-knockdown HCT-8 and HCT-8/5-FU cell lines. (B) Half maximal inhibitory concentration of FTO-knockdown and SIVA1 knockdown in HCT-8 and HCT-8/5-FU cell lines treated with 5-FU for 48 h. (C) Silencing SIVA1 increased cell growth by the CKK8 assay in FTO-knockdown HCT-8 and HCT-8/5-FU cell lines. (D) Silencing SIVA1 increased cell growth by the cell number in FTO-knockdown HCT-8 and HCT-8/5-FU cell lines. (E) Silencing SIVA1 rescued percentage of apoptotic in FTO-knockdown HCT-8 and HCT-8/5-FU cell lines by fluorescence-activated cell sorting. (F and G) Silencing SIVA1 rescued Bcl-2 expression level in FTO-knockdown HCT-8 and HCT-8/5-FU cell lines. Quantification of Bcl-2 expression was measured by ImageJ in (G). (H–J) Silencing SIVA1 decreased Caspase-3 activity by immunofluorescent assay in FTO-knockdown HCT-8 (H) and HCT-8/5-FU (I) cell lines treated with 5-FU for 24 h. The Ac-DEVD-CHO was used as a reversible inhibitor of Caspase-3. Quantification was measured by Imaris in (J).

(K–M) Silencing SIVA1 effectively alleviated FTO-dependent MC38 cell growth and increased resistance to 5-FU *in vivo* (K). Tumor growth curve (L) and tumor weight (M) are shown, n = 6. Data information: In all relevant panels, ns, not significant, *p < 0.05; **p < 0.01; ***p < 0.001; ****p < 0.0001; two-tailed t test. Data are presented as means ± SD and are representative of three independent experiments.

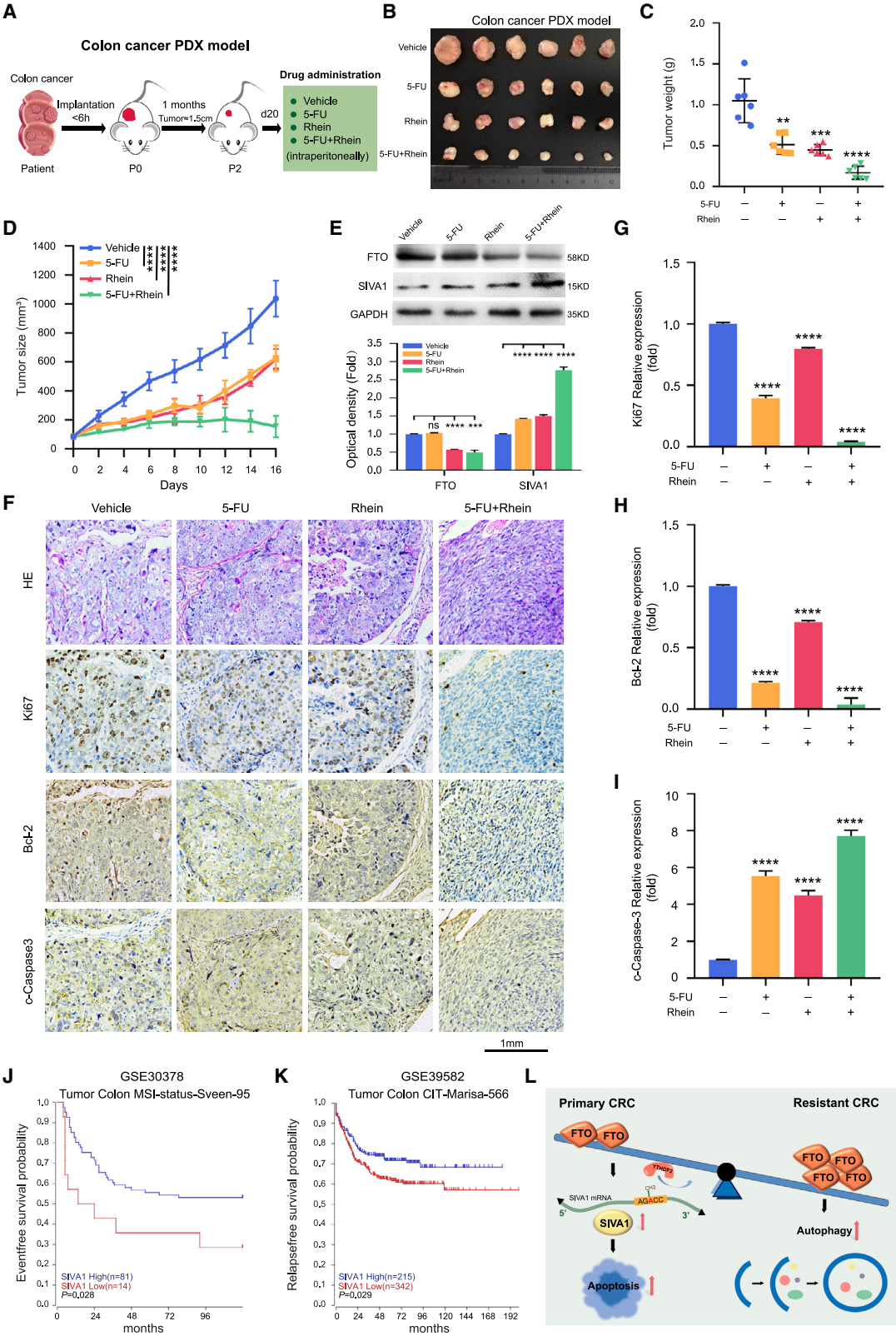


*(legend on next page)*

synthesized by using the PrimeScript RT reagent Kit (RR036A, Takara, Japan). The resulting cDNA was used for quantitative RT-PCR by using SYBR-Green Master mix (RR820B, Takara, Japan) in 7500 apparatus (Applied Biosystems). RT-PCR primer sequences are listed in Table S1.

#### Immunohistochemistry

For IHC analysis, CRC tissue slides were deparaffinized, rehydrated through an alcohol series followed by antigen retrieval with sodium citrate buffer. Tumor sections were blocked with 5% normal goat serum (Vector) with 0.1% Triton X-100 and 3% $H_2O_2$ in PBS for 60 min at room temperature and then incubated with appropriate primary antibodies 4°C overnight. IHC staining was performed with horseradish peroxidase (HRP) conjugates using DAB detection. Nuclei were counterstained with Hoechst. Images were taken with Nikon microscope (Japan).

#### RNA m$^6$A dot blot assay

The 300 ng poly (A) RNAs were gradient-diluted and spotted onto a nylon membrane. The membranes were UV (245 nm) crosslinked, blocked, incubated with m$^6$A antibody and HRP conjugated anti-rabbit IgG, and subsequently washed with PBST, and subtracted in visualizer (4600, Tanon, China). The same gradient-diluted total RNAs were spotted on the membrane, stained with 0.2% methylene blue in 0.3M sodium acetate (pH 5.2) for 2 h, and washed with ribonuclease-free water for 30 min.

#### Half maximal inhibitory concentration assay

Cells were cultured in 96-well plates with fresh medium in 0.5–1 $\times$ 10$^4$ per well. The corresponding concentration of drug was given to cells after the cultured plates were placed for 24 h. After 24 or 48 h treated, Cell Counting Kit-8 (Dojindo, Japan) was used to measure drug sensitivity at 450 nm using a microplate reader (Thermo, USA) after incubating at 37°C for an additional 2 h.

#### Cell proliferation and apoptosis assays

For Cell Counting Kit-8 (CCK8) assay, cells were seeded at 1,000 cells per well in 96-well plates with fresh medium. Cell viability was assayed using Cell Counting Kit-8 (CK04, Dojindo, Japan) at the time in 0, 48, 72, 96, and 120 h. The microplates were incubated at 37°C for an additional 2 h. Absorbance was read at 450 nm using a microplate reader (ThermoFisher, USA).

For cell number assay, cells were seeded at 1,000 cells per well in 96-well plates with fresh medium. Cell numbers were counted at the time in 0, 48, 72, 96, and 120 h. The results were expressed as a ratio of the treated over untreated cells (as 100%).

For EdU (5-Ethynyl-2′-deoxyuridine) assay, logarithmic growth stage cells with treated or not were seeded in a 12-well plate with corresponding concentration of EdU reagent for 2 h. Cells were washed with PBS for 5 min twice, before incubating with 4% paraformaldehyde for 30 min. After washing with PBS for 5 min twice, samples were permeated with 0.3% Triton X-100 in PBS, and dyed with a reaction solution (C0075S, Beyotime, China). Images collected with $\times$20 and $\times$40 visions in Nikon microscopy.

For cell apoptosis assays, cells were performed using Annexin V-PI Apoptosis Detection Kit I (WLA001a, Wanleibio, China) according to the manufacturer's instruction, and followed by flow cytometry analysis (Beckman, USA).

#### Clonogenic assays and colonosphere formation assay

For clonogenic assay, cells were seeded into 6-well plates at a density of 5,000 cells with fresh cell culture medium. Then plates with cells were treated with chemo drugs after 24 h cultured and maintained the related drug concentration for 10 days. Then, the plates were treated with polyformaldehyde fixing solution and crystal violet staining solution (Beyotime, China), and the colony pictures were captured separately.

For colonosphere formation assay, cells were seeded into ultralow attachment plates (Corning) at a density of 10,000 viable cells/mL in a serum-free DMEM-F12 supplemented with 100$\times$ insulin, 20 ng/mL epidermal growth factor, and 20 ng/mL basic fibroblast growth factor (Sigma), and 0.4% BSA (Sigma) for 2 weeks until the colonosphere became visible.

#### IF and transmission electron microscopy

For IF staining, colon cells with related treated slides were incubated with different primary antibodies, and were subsequently incubated with secondary antibodies. Nuclei were counterstained with DAPI. Images were obtained by Nikon (Japan).

For transmission electron microscopy assay, Fluorouracil-resistant HCT-8 colon cells with or without shFTO treated with DMSO or 5-FU for 24 h. Then, cells were fixed with 3% glutaraldehyde in 0.1 mol/L phosphate buffer (pH 7.4), followed by the fixation with 1% $OsO_4$. After dehydration, 10-nm thin sections were prepared and stained with uranyl acetate and plumbous nitrate before examination under a JEM-1230 transmission electron microscope (JEOL, Tokyo, Japan). High-resolution digital images were acquired from a randomly selected 10 different fields for samples of each condition.

**Figure 7. Inhibition of FTO significantly enhanced the sensitivity to 5-FU in CRC patient-derived xenograft mouse models**

(A–D) Graphic illustration of human CRC-PDX mouse model and treatment with regimen in the green box. (B–D) Inhibition of FTO by Rhein enhanced the sensitivity of CRC-PDX tumors to 5-FU (B). Tumor growth curve (C) and tumor weight (D) are shown, n = 6. (E) Validation of SIVA1 expression in CRC-PDX tumors treated with FTO inhibitors. (F) H&E and immunohistochemical images of Ki67, Bcl-2, and c-Caspase-3 in CRC-PDX tumors. (G–I) Quantification of Ki67 (G), Bcl-2 (H), and c-Caspase-3 (I) in immunohistochemical images by IPP analysis. (J and K) Up-regulation of SIVA1 was highly associated with longer overall survival in CRC patients. (L) Working model. Data information: In all relevant panels, ns, not significant, *p < 0.05; **p < 0.01; ***p < 0.001; ****p < 0.0001; two-tailed t test. Data are presented as means ± SD.

### Caspase-3 activity assay

For alive cell Caspase-3 activity assays, cells were performed using GreenNuc Caspase-3 activity assay (C1168S, Beyotime, China) according to the manufacturer's instructions. Nuclei were counterstained with DAPI. Images were obtained by Nikon (Japan).

### m$^6$A-RNA immunoprecipitation assay

Me-RIP sequencing was performed by standard methods described previously.[36] In brief, total RNAs were isolated from stable FTO-knockdown HCT-8 cells and their corresponding shCtrl controls and chemically fragmented into around 100 nt. The fragmented RNA was incubated with m$^6$A antibody for immunoprecipitation according to the manufacturer's instruction (Me-RIP m$^6$A Kit, Merck Millipore, USA). Enrichment of m$^6$A containing mRNA was sent for high-throughput NGS sequencing and validated by quantitative RT-PCR.

### Animal experiments

All animal experiments were approved by the Animal Ethics Committee of Sun Yat-sen University (SYSU-IACUC-2020-B1041). For the subcutaneous tumor mouse model in Dox-FTO group, $1 \times 10^7$ Dox-shCtrl, Dox-shFTO stable HCT8/5-FU or HCT-116 cell lines were injected into 5-week-old BALB/C nude mice and drug administration was adopted when the tumors reached about 100 mm$^3$ in size. Doxycycline hyclate was administered to mice via drinking water at a concentration of 2 mg/mL in 2% sucrose solution. For the subcutaneous tumor mouse model in shFTO group, $5 \times 10^5$ shCtrl, shFTO-1, shFTO-2 stable MC38 cells were injected into 5-week-old male C57BL/6 mice and drug administration was adopted after 48 h. For the subcutaneous tumor mouse model in shFTO&shSIVA1 group, $5 \times 10^5$ shCtrl, shFTO, shFTO&shSIVA1 stable MC38 cells were injected into 5-week-old male C57BL/6 mice and drug administration was adopted after 48 h. Drug administration (intraperitoneally): DMSO or 5-FU (50 mg/kg every 2 days). For the subcutaneous tumor mouse model in the Rhein group, $5 \times 10^5$ MC38 cells were injected into 5-week-old male C57BL/6 mice. Drug administration was adopted when the tumors reached about 100 mm$^3$ in size. Drug administration (intraperitoneally): DMSO, 5-FU (50 mg/kg every 2 days) or Rhein (10 mg/kg every 2 days).

For the tumor metastasis mouse model, 5-week-old C57BL/6 mice were randomly grouped and injected with $5 \times 10^5$ Control or shFTO stable MC38 cells via tail vein. Drug administration was adopted after 48 h. Drug administration (intraperitoneally): DMSO, 5-FU (50 mg/kg every 2 days) or Rhein (10 mg/kg every 2 days). To detect lung metastasis, mice were killed 2 weeks after tumor cell injection. Lung tissues were harvested and fixed with 4% PFA for paraffin-embedded section and lung metastases were detected with Nikon microscopy. For tumor intraperitoneal mouse model, $2 \times 10^6$ Dox-shCtrl, Dox-shFTO stable HCT8/5-FU cells were injected into 5-week-old male BALB/C nude mice. Drug administration was adopted after 48 h. Drug administration (intraperitoneally): DMSO, 5-FU (50 mg/kg every 2 days) or FB23-2 (10 mg/kg every 2 days). For tumor intraperitoneal mouse model, $5 \times 10^5$ shCtrl, shFTO-1, shFTO-2 stable MC38 cells were injected into 5-week-old C57BL/6 mice. Drug administration was adopted after 48 h. Drug administration (intraperitoneally): DMSO, 5-FU (50 mg/kg every 2 days) or Rhein (10 mg/kg every 2 days).

For the patient-derived tumor xenograft model, PDX tumors were generated from colon cancer patients. Human colon tumor tissue was implanted within 5 hours, expanded, and sub-implanted into 5-week-old male BALB/C nude mice. Drug administration began 3 weeks after tumors reached about 100 mm$^3$ in size. Drug administration (intraperitoneally): DMSO or 5-FU (50 mg/kg every 2 days) or Rhein (10 mg/kg every 2 days). Tumor volumes were measured using a Vernier caliper and calculated using the following formula: volume (cm$^3$) = $L \times W^2/2$, with L and W representing the largest and smallest diameters, respectively.

### Bioinformatics analysis

The gene expression profile dataset was downloaded from Gene Expression Omnibus (GEO) database, and subsequently analyzed by R (Version 3.4, http://www.bioconductor.org) with edgeR package. Fold-change (FC) of gene expression was calculated with a cut-off of log2FC $\geq$ 1, log2FC $< -1$ and p value $< 0.05$. The online database about R2, a website of Genomics Analysis and Visualization Platform (http://hgserve1.amc.nl/cgibin/r2/main.cgi&species=hs) was applied to determine the clinical survival of the related genes. KEGG pathway enrichment analysis was performed to investigate the activated pathways of the differentially expressed genes, by applying online tool of DAVID Bioinformatics Resources 6.8 (http://david.ncifcrf.gov) and KOBAS.3.0 (http://kobas.cbi.pku.edu.cn/anno_iden.php). The Search Tool for the Retrieval of Interacting Genes (STRING) database (V10.5, http://string-db.org) was recruited to predict the potential interaction between SIVA1 and apoptosis genes.

### Statistical analysis

Means and SDs were analyzed using GraphPad prism 8.0. Two-tailed Student's t test was used to compare the statistical difference between indicated groups. Pearson analysis was used to analyze correlation between genes. Statistical significance was accepted for p values of <0.05.

## ETHICS APPROVAL

All procedures followed were in accordance with the ethical standards of the Animal Care and Use Committee of Sun Yat-sen University. All institutional and national guidelines for the care and use of laboratory animals were followed.

## AVAILABILITY OF DATA AND MATERIAL

All unique reagents generated in this study are available from the corresponding authors with a completed Materials Transfer Agreement.

## SUPPLEMENTAL INFORMATION

Supplemental information can be found online at https://doi.org/10.1016/j.ymthe.2022.10.012.

## ACKNOWLEDGMENTS

We thank Dr. Dongshi Chen from the University of Pittsburgh for helpful discussions. This work was supported in part by grants from the National Natural Science Foundation of China (82122069, 82073869, 21672266, 81973174, 81701834, 81871994, 82022037, 31800993); Guangdong Basic and Applied Basic Research Foundation (2021B 1515020004, 2019A050510019, 2019B151502063); Guangdong Provincial Key Laboratory of Construction Foundation (2017B030314030, 2020B1212060034); Guangzhou Science and Technology Planning Program (202002020051, 201902020018); National Engineering Research Center for New Drug and Druggability Evaluation, Seed Program of Guangdong Province (2017B090903004); and Local Innovative and Research Teams Project of Guangdong Pearl Talents Program (2017BT01Y093).

## AUTHOR CONTRIBUTIONS

G.W. generated conception and designed this study. Z.L., A.W., L.S., H.L., Y.N., Y.D., and S.Y. developed the methodology and performed the assays. Z.L., A.W., L.S., and Y.N. analyzed and interpreted the data. G.W., Q.W., X.Z., K.H., and W.H. provided administrative, technical, or material support. G.W. and Z.L. organized the data and wrote the manuscript. The study supervisors were G.W., W.H., K.H., and A.W. All authors reviewed the manuscript. All authors read and approved the final manuscript.

## DECLARATION OF INTERESTS

The authors declare no competing interests.

## REFERENCES

1. Siegel, R.L., Miller, K.D., Ann Goding, S., Fedewa, S.A., Butterly, L.F., Andrea, C., Cercek, A., Smith, R.A., and Jemal, A. (2017). Colorectal cancer statistics. CA Cancer J. Clin. *67*, 177–193.
2. Wolpin, B.M., Meyerhardt, J.A., Mamon, H.J., and Mayer, R.J. (2007). Adjuvant treatment of colorectal cancer. CA Cancer J. Clin. *57*, 168–185.
3. Ribeiro, I.B., de Moura, D.T., Thompson, C.C., and de Moura, E.G. (2019). Acute abdominal obstruction: colon stent or emergency surgery? An evidence-based review. World J. Gastrointest. Endosc. *11*, 193.
4. Baretti, M., and Azad, N.S. (2018). The role of epigenetic therapies in colorectal cancer. Curr Probl. Cancer *42*, 530–547.
5. Chen, H., Yao, J., Bao, R., Dong, Y., Zhang, T., Du, Y., Wang, G., Ni, D., Xun, Z., Niu, X., et al. (2021). Cross-talk of four types of RNA modification writers defines tumor microenvironment and pharmacogenomic landscape in colorectal cancer. Mol. Cancer *20*, 29.
6. Zhao, B.S., Roundtree, I.A., and He, C. (2017). Post-transcriptional gene regulation by mRNA modifications. Nat. Rev. Mol. Cell Biol. *18*, 31–42.
7. Liu, J., Yue, Y., Han, D., Wang, X., Fu, Y., Zhang, L., Jia, G., Yu, M., Lu, Z., Deng, X., et al. (2014). A METTL3–METTL14 complex mediates mammalian nuclear RNA N 6-adenosine methylation. Nat. Chem. Biol. *10*, 93–95.
8. Ping, X.L., Sun, B.F., Lu, W., Xiao, W., Yang, X., Wang, W.J., Adhikari, S., Shi, Y., Lv, Y., Chen, Y.S., et al. (2014). Mammalian WTAP is a regulatory subunit of the RNA N6-methyladenosine methyltransferase. Cell Res. *24*, 177–189.
9. Jia, G., Fu, Y., Zhao, X., Dai, Q., Zheng, G., Yang, Y., Yi, C., Lindahl, T., Pan, T., Yang, Y.G., and He, C. (2011). N6-methyladenosine in nuclear RNA is a major substrate of the obesity-associated FTO. Nat. Chem. Biol. *7*, 885–887.
10. Zheng, G., Dahl, J.A., Niu, Y., Fedorcsak, P., Huang, C.M., Li, C.J., Vågbø, C.B., Shi, Y., Wang, W.L., Song, S.H., et al. (2013). ALKBH5 is a mammalian RNA demethylase that impacts RNA metabolism and mouse fertility. Mol. Cel. *49*, 18–29.
11. Liu, N., Dai, Q., Zheng, G., He, C., Parisien, M., and Pan, T. (2015). N 6-methyladenosine-dependent RNA structural switches regulate RNA–protein interactions. Nature *518*, 560–564.
12. Alarcon, C.R., Goodarzi, H., Lee, H., Liu, X., and Tavazoie, S. (2015). HNRNPA2B1 is a mediator of m6A-dependent nuclear RNA processing events. Cell *162*, 1299–1308.
13. Huang, H., Weng, H., Sun, W., Qin, X., Shi, H., Wu, H., Zhao, B.S., Mesquita, A., Liu, C., Yuan, C.L., et al. (2018). Recognition of RNA N 6-methyladenosine by IGF2BP proteins enhances mRNA stability and translation. Nat. Cell Biol. *20*, 285–295.
14. Hämmerle, M., Gutschner, T., Uckelmann, H., Ozgur, S., Fiskin, E., Gross, M., Skawran, B., Geffers, R., Longerich, T., Breuhahn, K., et al. (2013). Posttranscriptional destabilization of the liver-specific long noncoding RNA HULC by the IGF2 mRNA-binding protein 1 (IGF2BP1). Hepatology *58*, 1703–1712.
15. Wang, X., Lu, Z., Gomez, A., Hon, G.C., Yue, Y., Han, D., Fu, Y., Parisien, M., Dai, Q., Jia, G., et al. (2014). N6-methyladenosine-dependent regulation of messenger RNA stability. Nature *505*, 117–120.
16. Wang, X., Zhao, B.S., Roundtree, I.A., Lu, Z., Han, D., Ma, H., Weng, X., Chen, K., Shi, H., and He, C. (2015). N6-methyladenosine modulates messenger RNA translation efficiency. Cell *161*, 1388–1399.
17. Niu, Y., Wan, A., Lin, Z., Lu, X., and Wan, G. (2018). N(6)-Methyladenosine modification: a novel pharmacological target for anti-cancer drug development. Acta Pharm. Sin. B *8*, 833–843.
18. Lan, Q., Liu, P.Y., Haase, J., Bell, J.L., Hüttelmaier, S., and Liu, T. (2019). The critical role of RNA m(6)A methylation in cancer. Cancer Res. *79*, 1285–1292.
19. Shriwas, O., Priyadarshini, M., Samal, S.K., Rath, R., Panda, S., Kumar, S., Majumdar, D., Kumar Muduly, D., Botlagunta, M., and Dash, R. (2020). DDX3 modulates cisplatin resistance in OSCC through ALKBH5-mediated m(6)A-demethylation of FOXM1 and NANOG. Apoptosis *253-4*, 233–246.
20. Jin, D., Guo, J., Wu, Y., Du, J., Yang, L., Wang, X., Di, W., Hu, B., An, J., Kong, L., et al. (2019). m(6)A mRNA methylation initiated by METTL3 directly promotes YAP translation and increases YAP activity by regulating the MALAT1-miR-1914-3p-YAP axis to induce NSCLC drug resistance and metastasis. J. Hematol. Oncol. *12*, 135.
21. Yang, S., Wei, J., Cui, Y.H., Park, G., Shah, P., Deng, Y., Aplin, A.E., Lu, Z., Hwang, S., He, C., and He, Y.Y. (2019). m(6)A mRNA demethylase FTO regulates melanoma tumorigenicity and response to anti-PD-1 blockade. Nat. Commun. *10*, 2782.
22. Taketo, K., Konno, M., Asai, A., Koseki, J., Toratani, M., Satoh, T., Doki, Y., Mori, M., Ishii, H., and Ogawa, K. (2018). The epitranscriptome m6A writer METTL3 promotes chemo- and radioresistance in pancreatic cancer cells. Int. J. Oncol. *52*, 621–629.
23. Lin, Z., Niu, Y., Wan, A., Chen, D., Liang, H., Chen, X., Sun, L., Zhan, S., Chen, L., Cheng, C., et al. (2020). RNA m(6) A methylation regulates sorafenib resistance in liver cancer through FOXO3-mediated autophagy. EMBO J. *39*, e103181.
24. Ni, W., Yao, S., Zhou, Y., Liu, Y., Huang, P., Zhou, A., Liu, J., Che, L., and Li, J. (2019). Long noncoding RNA GAS5 inhibits progression of colorectal cancer by interacting with and triggering YAP phosphorylation and degradation and is negatively regulated by the m(6)A reader YTHDF3. Mol. Cancer *18*, 143.
25. Li, T., Hu, P.S., Zuo, Z., Lin, J.F., Li, X., Wu, Q.N., Chen, Z.H., Zeng, Z.L., Wang, F., Zheng, J., et al. (2019). METTL3 facilitates tumor progression via an m(6)A-IGF2BP2-dependent mechanism in colorectal carcinoma. Mol. Cancer *18*, 112.
26. Zhu, W., Si, Yan., Xu, J., Lin, Y., Wang, J.Z., Cao, M., Sun, S., Ding, Q., Zhu, L., and Wei, J.F. (2020). Methyltransferase like 3 promotes colorectal cancer proliferation by stabilizing CCNE1 mRNA in an m6A-dependent manner. J. Cell Mol. Med. *24*, 3521–3533.
27. Chen, X., Xu, M., Xu, X., Zeng, K., Liu, X., Sun, L., Pan, B., He, B., Pan, Y., Sun, H., et al. (2020). METTL14 suppresses CRC progression via regulating N6-methyladenosine-dependent primary miR-375 processing. Mol. Ther. *28*, 599–612.
28. Speakman, J.R. (2010). FTO effect on energy demand versus food intake. Nature *464*, E1. discussion E2.
29. Mauer, J., Luo, X., Blanjoie, A., Jiao, X., Grozhik, A.V., Patil, D.P., Linder, B., Pickering, B.F., Vasseur, J.J., Chen, Q., et al. (2017). Reversible methylation of m6A m in the 5′ cap controls mRNA stability. Nature *541*, 371–375.

30. Pausova, Z., Syme, C., Abrahamowicz, M., Xiao, Y., Leonard, G.T., Perron, M., Richer, L., Veillette, S., Smith, G.D., Seda, O., et al. (2009). A common variant of the FTO gene is associated with not only increased adiposity but also elevated blood pressure in French Canadians. Circ. Cardiovasc. Genet. *2*, 260–269.

31. Wehr, E., Schweighofer, N., Möller, R., Giuliani, A., Pieber, T.R., and Obermayer-Pietsch, B. (2010). Association of FTO gene with hyperandrogenemia and metabolic parameters in women with polycystic ovary syndrome. Metabolism *59*, 575–580.

32. Keller, L., Xu, W., Wang, H.X., Winblad, B., Fratiglioni, L., and Graff, C. (2011). The obesity related gene, FTO, interacts with APOE, and is associated with Alzheimer's disease risk: a prospective cohort study. J. Alzheimers Dis. *23*, 461–469.

33. Niu, Y., Lin, Z., Wan, A., Chen, H., Liang, H., Sun, L., Wang, Y., Li, X., Xiong, X.F., Wei, B., et al. (2019). RNA N6-methyladenosine demethylase FTO promotes breast tumor progression through inhibiting BNIP3. Mol. Cancer *18*, 46.

34. Wang, Q., Chen, C., Ding, Q., Zhao, Y., Wang, Z., Chen, J., Jiang, Z., Zhang, Y., and Xu, G. (2019). METTL3-mediated m6A modification of HDGF mRNA promotes gastric cancer progression and has prognostic significance. Gut *69*, 1193–1205.

35. Chen, M., Wei, L., Law, C.T., Tsang, F.H.C., Shen, J., Cheng, C.L.H., Tsang, L.H., Ho, D.W.H., Chiu, D.K.C., Lee, J.M.F., et al. (2018). RNA N6-methyladenosine methyltransferase-like 3 promotes liver cancer progression through YTHDF2-dependent posttranscriptional silencing of SOCS2. Hepatology *67*, 2254–2270.

36. Sun, L., Wan, A., Zhou, Z., Chen, G., Liang, H., Liu, C., Yan, S., Niu, Y., Lin, Z., and Zhan, S. (2020). RNA-binding protein RALY reprogrammes mitochondrial metabolism via mediating miRNA processing in colorectal cancer. Gut *70*, 1698–1712.

37. Li, Z., Weng, H., Su, R., Weng, X., Zuo, Z., Li, C., Huang, H., Nachtergaele, S., Dong, L., Hu, C., et al. (2017). FTO plays an oncogenic role in acute myeloid leukemia as a N6-methyladenosine RNA demethylase. Cancer Cell *31*, 127–141.

38. Cui, Q., Shi, H., Ye, P., Li, L., Qu, Q., Sun, G., Sun, G., Sun, G., Huang, Y., and He, C. (2017). m6A RNA methylation regulates the self-renewal and tumorigenesis of glioblastoma stem cells. Cell Rep. *18*, 2622–2634.

39. Su, R., Li, C., Dong, L., Li, C., Qing, Y., Deng, X., Wang, Y., Wang, X., Hu, C., and Yu, M. (2018). R-2HG exhibits anti-tumor activity by targeting FTO/m6A/MYC/CEBPA signaling. Cell *172*, 90–105.e123.

40. Yan F, A., Zhang, Z., Al-Kali, A., Liu, J., Pang, J., Zhao, N., He, C., Litzow, R.M., and Liu, S. (2018). A dynamic N 6-methyladenosine methylome regulates intrinsic and acquired resistance to tyrosine kinase inhibitors. Cell Res. *28*, 1062.

41. Ruan, D.Y., Li, T., Wang, Y.N., Meng, Q., Li, Y., Yu, K., Wang, M., Lin, J.F., Luo, L.Z., Wang, D.S., et al. (2021). FTO downregulation mediated by hypoxia facilitates colorectal cancer metastasis. Oncogene *40*, 5168–5181. https://doi.org/10.1038/s41388-021-01916-0.

42. Relier, S., Ripoll, J., Guillorit, H., Amalric, A., Achour, C., Boissière, F., Vialaret, J., Attina, A., Debart, F., Choquet, A., et al. (2021). FTO-mediated cytoplasmic m(6)Am demethylation adjusts stem-like properties in colorectal cancer cell. Nat. Commun. Commun. *12*, 1716. https://doi.org/10.1038/s41467-021-21758-4.

43. Wang, J., Qiao, Y., Sun, M., Sun, H., Xie, F., Chang, H., Wang, Y., Song, J., Lai, S., Yang, C., et al. (2022). FTO promotes colorectal cancer progression and chemotherapy resistance via demethylating G6PD/PARP1. Clin. Transl. Med. *12*, e772. https://doi.org/10.1002/ctm2.772.

44. Chen, B., Ye, F., Yu, L., Jia, G., Huang, X., Zhang, X., Peng, S., Chen, K., Wang, M., Gong, S., et al. (2012). Development of cell-active N 6-methyladenosine RNA demethylase FTO inhibitor. J. Am. Chem. Soc. *134*, 17963–17971.

45. Huang, Y., Su, R., Sheng, Y., Dong, L., Dong, Z., Xu, H., Ni, T., Zhang, Z.S., Zhang, T., Li, C., et al. (2019). Small-molecule targeting of oncogenic FTO demethylase in acute myeloid leukemia. Cancer cell *35*, 677–691.e10.

46. Peng, S., Xiao, W., Ju, D., Sun, B., Hou, N., Liu, Q., Wang, Y., Zhao, H., Gao, C., Zhang, S., et al. (2019). Identification of entacapone as a chemical inhibitor of FTO mediating metabolic regulation through FOXO1. Sci. Transl. Med. *11*, eaau7116.

47. Su, R., Dong, L., Li, Y., Gao, M., Han, L., Wunderlich, M., Deng, X., Li, H., Huang, Y., Gao, L., et al. (2020). Targeting FTO suppresses cancer stem cell maintenance and immune evasion. Cancer Cell *38*, 79–96.e11.

48. Liu, J., Eckert, M.A., Harada, B.T., Liu, S.M., Lu, Z., Yu, K., Tienda, S.M., Chryplewicz, A., Zhu, A.C., Yang, Y., et al. (2018). m 6 A mRNA methylation regulates AKT activity to promote the proliferation and tumorigenicity of endometrial cancer. Nat. Cell Biol. *20*, 1074–1083.

49. Yu, T.C., Yu, Y., Guo, F., Yu, Y., Sun, T., Ma, D., Han, J., Zou, W., and Fang, Y.J. (2017). Fusobacterium nucleatum promotes chemoresistance to colorectal cancer by modulating autophagy. Cell *170*, 548–563.e16.

50. Wei, Y., Becker, N., Zou, Z., Becker, N., Anderson, M., Sumpter, R., Xiao, G., Kinch, L., Kpduru, P., Levine, B., et al. (2013). EGFR-mediated Beclin 1 phosphorylation in autophagy suppression, tumor progression, and tumor chemoresistance. Cell *154*, 1269–1284.

51. Ou, J., Peng, Y., Yang, W., Zhang, Y., Hao, J., Li, F., Chen, Y., Zhao, Y., Xie, X., Wu, S., et al. (2019). ABHD5 blunts the sensitivity of colorectal cancer to fluorouracil via promoting autophagic uracil yield. Nat. Commun. *10*, 1078.

52. Zhang, L., Li, J., Ouyang, L., Liu, B., and Cheng, Y. (2016). Unraveling the roles of Atg4 proteases from autophagy modulation to targeted cancer therapy. Cancer Lett. *373*, 19–26.

53. Xue, L., Chu, F., Cheng, Y., Sun, X., Borthakur, A., Ramarao, M., Pandey, P., Wu, M., Schlossman, S.F., and Prasad, K.V.S. (2002). Siva-1 binds to and inhibits BCL-XL-mediated protection against UV radiation-induced apoptosis. Proc. Natl. Acad. Sci. USA *99*, 6925–6930.

54. Prasad, K.V.S., Ao, Z., Yoon, Y., Wu, M.X., Rizk, M., Jacquot, S., and Schlossman, S.F. (1997). CD27, a member of the tumor necrosis factor receptor family, induces apoptosis and binds to Siva, a proapoptotic protein. Proc. Natl. Acad. Sci. USA *94*, 6346–6351.

55. Jacobs S, Murray, J.I., Basak, S., PathakL, N., and Attardi, D. (2007). Siva is an apoptosis-selective p53 target gene important for neuronal cell death. Cell Death Differ. *14*, 1374.

56. Hou, G., Li, L., Li, L., Yang, Q., Liu, X., Huang, C., Lu, R., Chen, R., Wang, Y., and Jiang, B. (2021). SUMOylation of YTHDF2 promotes mRNA degradation and cancer progression by increasing its binding affinity with m6A-modified mRNAs. Nucleic Acids Res. *49*, 2859–2877.

57. Li, J., Xie, H., Ying, Y., Chen, H., Yan, H., He, L., Xu, M., Xu, X., Liang, Z., Liu, B., et al. (2020). YTHDF2 mediates the mRNA degradation of the tumor suppressors to induce AKT phosphorylation in N6-methyladenosine-dependent way in prostate cancer. Mol. Cancer *19*, 152.

58. Chai, R.C., Chang, Y.Z., Chang, X., Pang, B., An, S.Y., Zhang, K.N., Chang, Y.H., Jiang, T., and Wang, Y.Z. (2021). YTHDF2 facilitatesUBXN1mRNA decay by recognizing METTL3-mediated m6A modification to activate NF-κB and promote the malignant progression of glioma. J. Hematol. Oncol. *14*, 109.

59. Niu, Y., Lin, Z., Wan, A., Sun, L., Yan, S., Liang, H., Zhan, S., Chen, D., Bu, X., Liu, P., et al. (2021). Loss-of-function genetic screening identifies ALDOA as an essential driver for liver cancer cell growth under hypoxia. Hepatology *74*, 1461–1479.